Understanding the Seeding Pulse-Induced Optical Amplification in N_2^+ Pumped by 800 NM Femtosecond Laser Pulses

Zhengquan Fan [1], Xiang Zhang [1], Qi Lu [1], Yu Luo [1], Qingqing Liang [1], Luqi Yuan [2] ![ORCID], Zhedong Zhang [3] and Yi Liu [1,4],* ![ORCID]

[1] Shanghai Key Lab of Modern Optical System, University of Shanghai for Science and Technology, 516, Jungong Road, Shanghai 200093, China; 191380042@st.usst.edu.cn (Z.F.); 181390040@st.usst.edu.cn (X.Z.); 201310033@st.usst.edu.cn (Q.L.); 192380318@st.usst.edu.cn (Y.L.); qqliang@usst.edu.cn (Q.L.)

[2] School of Physics and Astronomy, Shanghai Jiao Tong University, Shanghai 200240, China; yuanluqi@sjtu.edu.cn

[3] Department of Physics, City University of Hong Kong, Kowloon, Hong Kong SAR, China; zzhan26@cityu.edu.hk

[4] CAS Center for Excellence in Ultra-intense Laser Science, Shanghai 201800, China

* Correspondence: yi.liu@usst.edu.cn; Tel.: +86-021-5527-1309

Abstract: Nitrogen ions pumped by intense femtosecond laser pulses present an optical gain at 391.4 nm, evident by energy amplification of an injected resonant seeding pulse. We report a time-resolved measurement of the amplification process with seeding pulses having varying intensities. It is found that the amplification factor depends on the intensity of the seeding pulse and the effective temporal window for the optical gain becomes longer by applying more intense seeding pulses. These two features are in sharp contrast with classic pump-probe experiments, pinpointing the crucial role of macroscopic coherence and its dynamics during the lasing process. We further measure the temporal profile of the amplified emission for seeding pulse injected at different time delays. A complicated temporal behavior is observed, which highlights the nature of the superfluorescence.

Keywords: superfluorescence; optical amplification; air lasing

1. Introduction

Nitrogen molecules in ambient air pumped by intense femtosecond laser pulses emit coherent radiation at 391.4 nm and 427.8 nm in the forward direction [1–9]. These two wavelengths correspond to the $B^2\Sigma_u^+(v'=0) - X^2\Sigma_g^+(v=0,\ 1)$ transition of ionic nitrogen molecules, where v' and v are the vibration quantum number of the upper and lower electronic levels. This forward coherent emission was first discovered using mid-infrared pump pulse tuned between 1.1 to 2.6 μm [1]. Later, it was observed with pump pulses at other wavelengths, including 1.5 μm [2], 1.03 μm [3], 800 nm [4–8], as well as 400 nm [9]. Very recently, X. Zhang et al. reported that backward emission at 391.4 nm can also be observed by optimizing the focal geometry [10]. These coherent emissions from nitrogen ions, together with those from excited neutral nitrogen molecules [11–13], Ar atoms [14], as well as photon-dissociated O atoms [15,16] and N atoms [17], have been coined as "air lasing" with the view that ambient air or the main components of air serve as the medium for optical gain in a cavity-free manner. Air lasing has drawn much attention over the past 10 years since it holds the unique potential to generate coherent optical beams from the sky to the ground, which may open the door for remote optical sensing with coherent laser spectroscopy [18–20]. Among the different methods of air lasing,

the lasing action of N_2^+ has been extensively investigated due to the rich physics involved. At present, the origin of the optical gain of N_2^+ is still under debate and many different interpretations have been proposed [1,5–8,21–25].

Examination of this optical gain in the temporal domain has provided valuable insights into the underlying mechanism [7]. This is done by injecting an external seeding pulse into the nitrogen gas plasma after the main pump pulse. In the first measurement of the temporal dynamics of the optical gain, it was found that the optical gain lasts for more than 100 ps, under the experimental condition of 180 mbar nitrogen gas, incident pulse energy of E_{in} = 1.9 mJ focused by a lens with focal length f = 40 cm [7]. Later, under similar experimental conditions, the optical gain was found to last for less than 10 ps [26,27], in an obvious contradiction with the earlier results. Recently, Britton and co-workers performed the gain dynamics measurement for gas cell and gas jet [28]. They reported that the decay process of the gain depends sensitively on the concentration of the N_2. The underlying reasons for these above contradictory experimental observations remain unclear.

So far, the physics of this gain dynamics measurement was understood in the framework of classic pump-probe experiments, where the probe pulse measures the optical gain within a leading-order assumption, i.e., the probe pulse is weak enough and does not affect the temporal evolution of the optical gain and the lasing process. However, recent experimental evidences have shown that this 391.4 nm emission is of the nature of superfluorescence, a cooperative radiation process where the built up of macroscopic coherence plays a crucial role [27,29]. In particular, it has been observed that the probe pulse stimulates the macroscopic coherence and accelerates the 391.4 nm emission in real-time domain [27]. Therefore, the seed pulse should no longer be considered a weak probe as in classic pump-probe experiments. Its role in the development of the gain dynamics and lasing process needs to be clarified.

In this work, we report on measurements of the amplification ratios, the gain dynamics, as well as the temporal profile of the lasing signal with varying seeding pulses intensities. We find that the amplification factor, and thus the optical gain g, depends on the intensity of the incident seeding pulse. Moreover, it is observed that more intense seeding pulse leads to a longer temporal window of optical gain. These evidently highlight the distinction of the seeding pulse from a probe in classic pump-probe experiments. To gain insight into the amplified signal at different pump-seeding delays τ_{P-S}, we further examine the temporal profile of the lasing signal for different delays between the pulse and seeding pulses. A strong and accelerated emission is observed for short τ_{P-S} less than 8 ps. The above features can be understood in the framework of superfluorescence, instead of a classic pump-probe technique.

2. Experimental Setup

In our experiments, femtosecond laser pulses from a Ti: Sapphire Chirped Pulses Amplification system is used. The laser system delivers 35 fs laser pulses with central wavelength at 796 nm and maximum pulse energy of 12 mJ at a 1 kHz repetition rate. The beam diameter is about 11 mm at $1/e^2$ level of fluence. The main experimental setup is schematically shown in Figure 1. The laser beam was first split into three arms by two dielectric beam splitters. One beam with pulse energy of 1.9 mJ was used as the pump pulse to generate a plasma filament in nitrogen gas. Pulses of second arm are up-converted in a β-BBO crystal to generate its second harmonic with central wavelength around 398 nm. A 10-nm bandwidth interference filter was used to select a seeding pulse around 390 nm. The seeding pulse was adjusted to have a horizontal polarization, parallel to that of the pump beam. The temporal delay τ_{P-S} between the pump and seeding pulse was controlled by a mechanical delay line. The co-propagating pump and seeding pulses are focused by a convex lens with a focal length of 30 cm. The focused pump laser creates a plasma channel inside the gas chamber filled with pure nitrogen at pressure of 50 mbar. The forward emission from the plasma is spectrally filtered by proper optical filters to eliminate the residual strong 800 nm pulse and the radiation below 450 nm was collected by a convex lens of f = 10 cm into the tip of an optical fiber connected to a spectrometer.

To perform time-resolved measurements of the lasing emission, the forward 391.4 nm emission and a third weak 796 nm probe pulses are focused together onto a sum frequency generation BBO crystal to produce an optical signal at 263 nm. Recording the 263 nm signal as a function of the delay between the 391.4 nm optical signal and the probe pulse provide a cross-correlation measurement of the forward lasing emission.
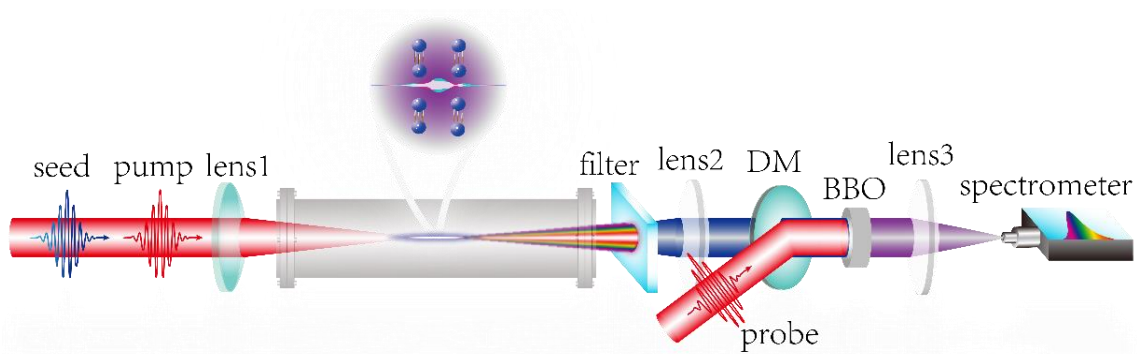

Figure 1. Experimental setup. The femtosecond laser pulses are focused by an f = 30 cm into the gas chamber to form a plasma filament. To measure the gain dynamics, the emission from the plasma is collected into a fiber spectrometer after proper filtering. For time-resolved measurement, the forward 391.4 nm emission and the probe pulse are focused onto the sum-frequency generation BBO crystal and the SFG signal at 263 nm are recorded as a function of the delay between the 391.4 nm emission and the probe pulse. (DM: dichroic mirror).

3. Results

In Figure 2a, we first present the amplification of an external seeding pulse injected inside the nitrogen gas plasma. The lasing emission produced by the pump pulse itself is not strong in this case. When the seeding pulse (gray line) was injected at a proper time delay, a significant amplification can be observed at 391.4 nm (red line). The amplification ratio, defined as $S = I_{amp}/I_{seed}$, is 38 for this result. Here I_{amp} and I_{seed} denote the spectral intensity of the 391.4 nm spectral component after amplification and that of the seeding pulse, respectively. We then measured the amplified 391.4 nm signal as a function of the spectral intensity of the seeding pulse, as presented in Figure 2b (black line). By increasing the seed pulse intensity, the amplified 391.4 nm emission is seen to be strongly enhanced. In the meantime, we notice that the amplification tends to saturate when gradually increasing the seed intensity. The amplification factor as a function of the seeding pulse intensity is also presented in Figure 2b (red line). The amplification factor is of the order of 10,000 for weak seed pulse, while it decreases rapidly until close to ~100 by increasing the seeding pulse intensity.
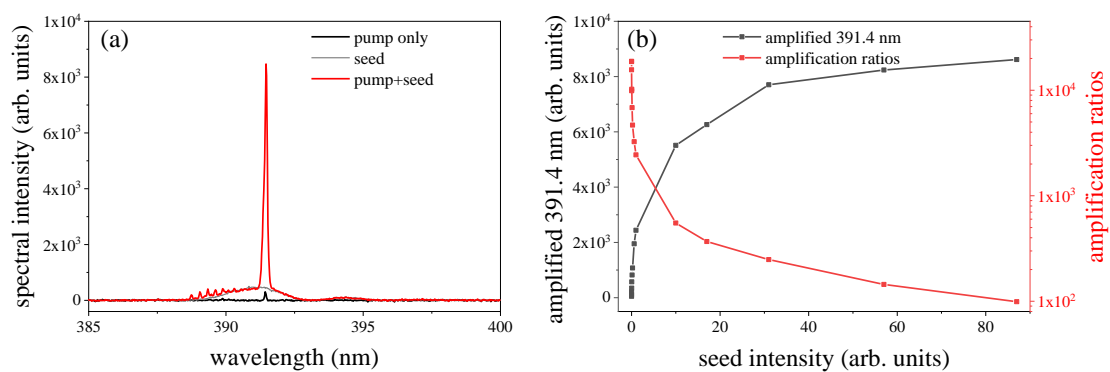

Figure 2. (**a**) Spectra of the 391.4 nm emission obtained in the presence of the pump pulse only (black), and both pump and seeding pulses (red). The spectrum of the seeding pulse is also shown (gray). (**b**) The spectral intensity of the amplified 391.4 nm signal (black), the amplification ratio as a function of the seeding pulse spectral intensity (red).

We further measured the 391.4 nm gain dynamics with various spectral intensities of seed pulse. The experimental results are presented in Figure 3. The intensity ratio of the seed pulse in Figure 3a–d is 78.1: 0.52: 0.12: 0.006. For strong seeding pulse, the effective temporal window for amplification τ_{gain} (defined as 10% of the maximum intensity) is long, close to 10 ps in Figure 3a. In contrast, this temporal window becomes less than 1 ps in the case of very weak seeding pulse, as depicted in Figure 3d. For intermediate intensity of the seeding pulse, τ_{gain} increases as the seeding pulse becomes stronger. These observations provide a clue for the contradictory results presented previously where different τ_{gain} have been reported under similar pumping conditions [7,26,27]. This is because the intensity of the seeding pulse can change in different experimental campaigns of the same group or vary significantly in experiments of different research groups.
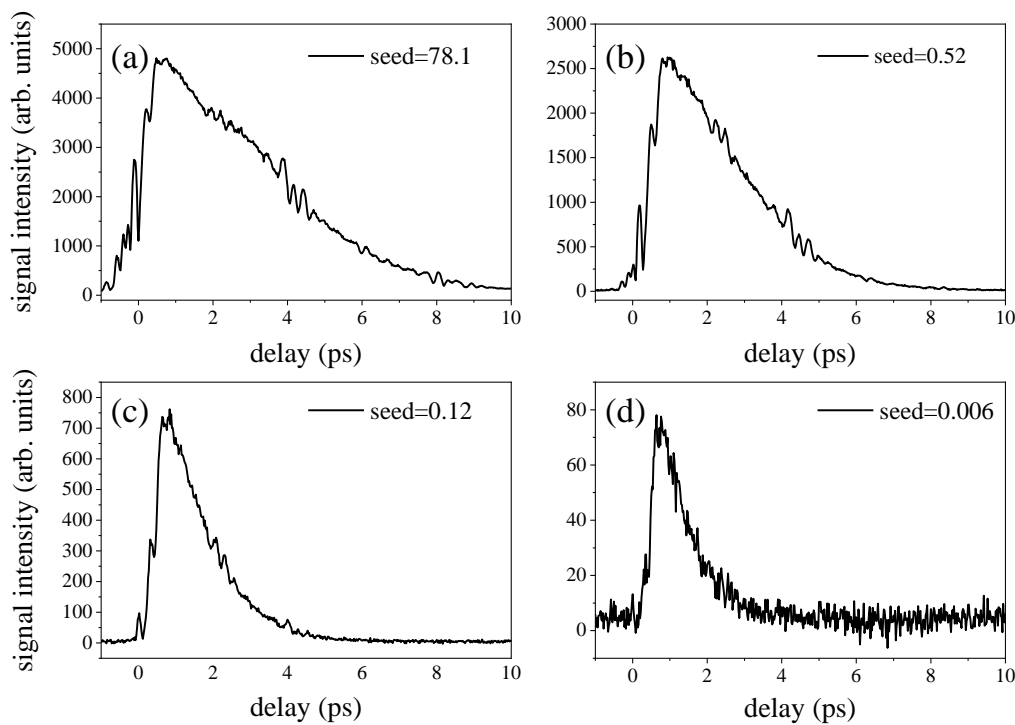

Figure 3. Amplified 391.4 nm signal as a function of the delay between pump and seeding pulses, for various energies of seeding pulses. The relative energies of the seeding pulse in (**a**–**d**) are 78.1: 0.52: 0.12: 0.006.

To gain insight into the temporal profile of the amplified emission at different τ_{P-S}, we performed the time-resolved measurements of the emission using cross-correlation method based on the sum-frequency generation inside a BBO crystal [26,29]. The results are displayed in Figure 4. The pump pulse is set at zero delay and eight different values of pump-seed delay τ_{P-S} have been chosen, where positive τ_{P-S} denotes the situation that the seeding pulse comes after the pump pulse. For negative delays where the seeding pulse irradiates the nitrogen gas before the 800 nm pump pulse, the seeding pulse has no influence on the 391.4 nm emission. The 391.4 nm emission created by the 800 nm pump itself reaches the maximum intensity ~3 ps after the pump pulse, giving rise to a pulse with duration of ~2 ps. When the seeding pulse comes slightly after the pump pulse ($\tau_{P-S} = 1$ ps), a strongly amplified emission is observed, with the built-up time being significantly suppressed. For increasing delay τ_{P-S}, the emission intensity decreases and the pulse becomes longer. For the situation where the seeding pulse substantially lags the pump pulse, i.e., $\tau_{P-S} = 11$ ps, it has no influence on the emission since the superfluorescence process already terminates before its arrival.
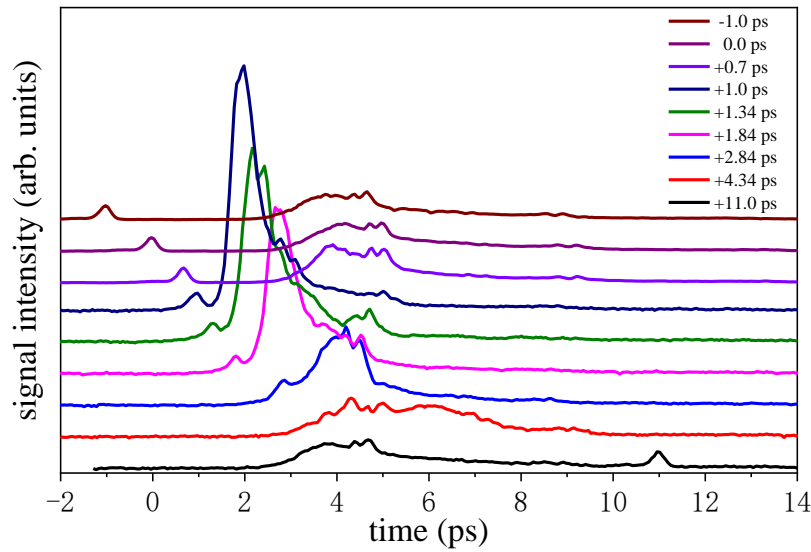
Figure 4. Temporal profile of the forward emission at 391.4 nm for different delays between the pump and seeding pulses. These measurements correspond to Figure 3b, where the seed intensity is 0.52 arb. units. The time delays between the pump and seeding pulse are listed in the figure. The zero delay along the horizontal axis is defined with respect to the 800 nm pump laser pulse.

4. Discussion

How should we understand the dependence of the effective gain lifetime τ_{gain} on the intensity of the seeding pulse? In a classic laser system without involving the coherence, the optical gain is directly proportional to the density of the molecules showing population inversion, $g = \Delta n B_{21} f(\nu) h\nu / c$. Here, $\Delta n = n_2 - n_1$ is the population inversion density, B_{21}, f(ν), h, ν are the Einstein coefficient, the lineshape of the considered transition, the Planck constant, and the transition frequency, respectively. In this case, an externally injected resonant seeding pulse does not affect the population dynamics. Therefore, the dynamics of the optical gain can be directly measured by recording the amplified laser energy as a function of the delay between the pump and seeding pulses [30,31].

In the current N_2^+ study, population inversion between the electronic states $B^2\Sigma_u^+$ and $X^2\Sigma_g^+$ is indicated to be unnecessary and the macroscopic coherence actually plays an essential role [24,32,33]. Time-resolved measurements have shown that the built-up time and the duration of the amplified 391.4 nm emission, as well as its peak intensity, present a characteristic dependence on gas pressure, indicating the superfluorescence nature [27,29]. Superfluorescence is divided into different regimes depending on several parameters, including the characteristic delay time τ_D and the collision dephasing time T_2, where a competition between the coherence build-up and the decoherence process is crucial [34,35]. It turns out that the injection of an external seeding pulse can accelerate and enhance the microscopic coherence [27,32,36], by means of a non-perturbative effect on the quantum dynamics of nitrogen ions. To understand qualitatively the behaviors in Figure 3, we adopt a two-level model for the N_2^+ system, where level 1 and level 2 refer to the ground state $X^2\Sigma_g^+$ and the excited state $B^2\Sigma_u^+$, respectively. We assume the initial populations $\rho_{11}(0)$ and $\rho_{22}(0)$ at t = 0 after the 800 nm pump pulse passes through the medium, whereas the initial coherence $\rho_{12}(0)$ can be properly neglected due to the weak superfluorescence without the seed. Let E_s(t) denote the envelope of the seeding pulse, and the molecule-field interaction is of the dipolar form $-\mu\left(E_s(t)e^{-i\omega t} + c.c.\right)/2$. Assuming the center frequency of the seeding field in resonance with the electronic transition, i.e., $\omega = \omega_{12}$, one can find the equation of motion for the density matrix under the rotating-wave approximation:

$$\frac{\partial \rho_{12}}{\partial t} = -i\omega\rho_{12} - i\frac{\wp E_s}{\hbar}(\rho_{11} - \rho_{22}) \tag{1}$$

where $\wp$ is the dipole moment. By defining $\rho_{12} = \sigma_{12}e^{-i\omega t}$ we have

$$\frac{\partial \sigma_{12}}{\partial t} = -i\frac{\wp E_s}{\hbar}(\rho_{11} - \rho_{22}) \tag{2}$$

The seeding field is ultrashort with a temporal width Δ. It locates at time τ_{P-S} with respect to the pump pulse. Given the seeding pulse of ~ 0.1 nJ level energy in our experiments, the peak electric field E_s is correspondingly of the order 10^7 V/m. As a result, the Rabi frequency $\wp E_s/\hbar$ is of the order 10^{11} s^{-1}, given the dipole moment $\wp \approx 6.6 \times 10^{-30}$ C·m between $B^2\Sigma_u^+$ and $X^2\Sigma_g^+$ states. In the limit $\wp E_s\Delta/\hbar \ll 1$, one can integrate Equation (2) up to the first-order expansion with the molecule-field coupling, and it follows the expression of the coherence after the passage of the seeding field ($t = \tau_{P-S} + \Delta$):

$$\sigma_{12}\left(\tau_{p-s} + \Delta\right) \approx -i\frac{\wp}{\hbar}\left[\rho_{11}\left(\tau_{p-s}\right) - \rho_{22}\left(\tau_{p-s}\right)\right]\int_{\tau_{ps}-\Delta}^{\tau_{ps}+\Delta} E_s(t')dt'e^{-i\omega\tau_{p-s}}$$
$$\propto \left[\rho_{11}\left(\tau_{p-s}\right) - \rho_{22}\left(\tau_{p-s}\right)\right]A \tag{3}$$

where $A = \int_{\tau_{p-s}-\Delta}^{\tau_{p-s}+\Delta} E_s(t')dt'$ is the area of the seeding pulse. Therefore, the amplitude of the coherence σ_{12} induced by the seeding pulse depends on the population distribution in the medium at the delay τ_{p-s} and the seeding field intensity.

It is known that in the superfluorescence, the characteristic delay time τ_D of the emission is inversely proportional to the macroscopic coherence in the system, i.e., $\tau_D \propto 1/\sigma_{12}$ [35,37]. Nevertheless, collision dephasing of the dipoles leads to decay of the coherence, as characterized by the dephasing time T_2. The superfluoresence can occur when the coherence is built up within the time τ_D before its decay by collisions, i.e., $\tau_D < T_2$ [35,37]. Therefore, one finds that with the injection of seeding pulse, the superfluorescence can be formed when $\sigma_{12} > const./T_2$. As a result, we can see that a stronger seeding pulse can lead to satisfaction of the above criterion at longer delay τ_{p-s}. This explains qualitatively the longer temporal window for the optical gain observed in experiments using more intense seeding pulses (Figure 3).

The above analysis shines new light on the understanding of the results shown in Figure 4. With negative τ_{p-s}, where the seeding pulse precedes the pump laser, the nitrogen ions give rise to superfluorescence, owing to the spontaneous emission photons from the plasma or the second harmonic generated inside the plasma. This superfluorescence peaks around ~3 ps and terminates around ~8 ps. When the seeding pulse enters the nitrogen plasma after its creation and before the accomplishments of the superfluorescence ($\tau_{p-s} < 8$ ps), the seeding pulse strongly enhances the superfluorescence, accompanied by a reduction of the superfluorescence, accompanied by a reduction of the τ_D. If the seeding pulses comes later than 8 ps in current experiments, it has no influence on the superfluorescence and induces no amplification since it can no longer provoke built-up of the macroscopic coherence.

5. Conclusions

In summary, we measured the amplified 391.4 nm emission from N_2^+ ions pumped by 800 nm femtosecond laser pulses, in the presence of an external seeding pulse having various intensities. Several features of this amplification process are revealed. (1) The experimentally deduced optical gain strongly depends on the seeding pulse intensity; (2) The "gain dynamics" named previously show a dependence on the intensity of the seeding pulse; (3) The amplified signal exhibits the temporal profiles varying with pump-seed delays. These observations provide a unified explanation for the results as to the gain dynamics causing ambiguity before. More importantly, they suggest that the seeding pulse here may not be considered a weak probe as in the classic pump-probe experiment, going much beyond the perturbative approach, which had been mostly studied before. Instead, a full consideration

of how the superfluorescence process is formed is necessary when one employs a seeding pulse in such experiments. This non-perturbative effects brings up a challenge for the theory, as a hard-core problem.

Author Contributions: Conceptualization, Y.L. (Yi Liu); software, Q.L. (Qingqing Liang); formal analysis, L.Y., Z.Z., and Y.L. (Yi Liu); investigation, Z.F., X.Z., Q.L. (Qi Lu), and Y.L. (Yu Luo); writing—Z.F., L.Y., Z.Z., and Y.L. (Yi Liu). All authors have read and agreed to the published version of the manuscript.

Conflicts of Interest: The authors declare no conflict of interest.

References

1. Yao, J.; Zeng, B.; Xu, H.; Li, G.; Chu, W.; Ni, J.; Zhang, H.; Chin, S.L.; Cheng, Y.; Xu, Z. High-brightness switchable multiwavelength remote laser in air. *Phys. Rev. A* **2011**, *84*, 051802. [CrossRef]

2. Azarm, A.; Corkum, P.; Polynkin, P. Optical gain in rotationally excited nitrogen molecular ions. *Phys. Rev. A* **2017**, *96*, 051401. [CrossRef]

3. Kartashov, D.; Möhring, J.; Andriukaitis, G.; Pugžlys, A.; Zheltikov, A.; Motzkus, M.; Baltuška, A. Stimulated amplification of UV emission in a femtosecond filament using adaptive control. In Proceedings of the CLEO, SAN Jose, CA, USA, 6–11 May 2012; p. QTh4E.6.

4. Liu, Y.; Brelet, Y.; Point, G.; Houard, A.; Mysyrowicz, A. Self-seeded lasing in ionized air pumped by 800 nm femtosecond laser pulses. *Opt. Express* **2013**, *21*, 22791–22798. [CrossRef] [PubMed]

5. Xu, H.; Lötstedt, E.; Iwasaki, A.; Yamanouchi, K. Sub-10-fs population inversion in N_2^+ in air lasing through multiple state coupling. *Nat. Commun.* **2015**, *6*, 8347. [CrossRef]

6. Zhong, X.; Miao, Z.; Zhang, L.; Liang, Q.; Lei, M.; Jiang, H.; Liu, Y.; Gong, Q.; Wu, C. Vibrational and electronic excitation of ionized nitrogen molecules in intense laser fields. *Phys. Rev. A* **2017**, *96*, 043422. [CrossRef]

7. Yao, J.; Li, G.; Jing, C.; Zeng, B.; Chu, W.; Ni, J.; Zhang, H.; Xie, H.; Zhang, C.; Li, H.; et al. Remote creation of coherent emissions in air with two-color ultrafast laser pulses. *New J. Phys.* **2013**, *15*, 023046. [CrossRef]

8. Arissian, L.; Kamer, B.; Rastegari, A.; Villeneuve, D.M.; Diels, J.C. Transient gain from N_2^+ in light filaments. *Phys. Rev. A* **2018**, *98*, 053438. [CrossRef]

9. Wang, T.J.; Daigle, J.F.; Ju, J.; Yuan, S.; Li, R.; Chin, S.L. Forward lasing action at multiple wavelengths seeded by white light from a femtosecond laser filament in air. *Phys. Rev. A* **2013**, *88*, 053429. [CrossRef]

10. Zhang, X.; Danylo, R.; Fan, Z.; Ding, P.; Kou, C.; Liang, Q.; Houard, A.; Tikhonchuk, V.; Mysyrowicz, A.; Liu, Y. Backward lasing of singly ionized nitrogen ions pumped by femtosecond laser pulses. *Appl. Phys. B* **2020**, *126*, 53. [CrossRef]

11. Kartashov, D.; Ališauskas, S.; Andriukaitis, G.; Pugžlys, A.; Shneider, M.; Zheltikov, A.; Chin, S.L.; Baltuška, A. Free-space nitrogen gas laser driven by a femtosecond filament. *Phys. Rev. A* **2012**, *86*, 033831. [CrossRef]

12. Mitryukovskiy, S.; Liu, Y.; Ding, P.; Houard, A.; Mysyrowicz, A. Backward stimulated radiation from filaments in nitrogen gas and air pumped by circularly polarized 800 nm femtosecond laser pulses. *Opt. Express* **2014**, *22*, 12750–12759. [CrossRef] [PubMed]

13. Ding, P.; Oliva, E.; Houard, A.; Mysyrowicz, A.; Liu, Y. Lasing dynamics of neutral nitrogen molecules in femtosecond filaments. *Phys. Rev. A* **2016**, *94*, 043824. [CrossRef]

14. Dogariu, A.; Miles, R.B. Three-photon femtosecond pumped backwards lasing in argon. *Opt. Express* **2016**, *24*, A544–A552. [CrossRef]

15. Dogariu, A.; Michael, J.B.; Scully, M.O.; Miles, R.B. High-gain backward lasing in air. *Science* **2011**, *331*, 442–445. [CrossRef] [PubMed]

16. Laurain, A.; Scheller, M.; Polynkin, P. Low-threshold bidirectional air lasing. *Phys. Rev. Lett.* **2014**, *113*, 253901. [CrossRef] [PubMed]

17. Dogariu, A.; Miles, R. Backwards nitrogen double lasing in air for remote trace detection. In Proceedings of the Imaging and Application Optics, OSA, Seattle, DC, USA, 13–17 July 2014; p. LW2D.3.

18. Malevich, P.N.; Maurer, R.; Kartashov, D.; Ališauskas, S.; Lanin, A.A.; Zheltikov, A.M.; Marangoni, M.; Cerullo, G.; Baltuška, A.; Pugžlys, A. Stimulated Raman gas sensing by backward UV lasing from a femtosecond filament. *Opt. Lett.* **2015**, *40*, 2469–2472. [CrossRef]

19. Bood, J.; Aldén, M. Diagnostic Properties of Two-Photon-Pumped Stimulated Emission in Atmospheric Species. In *Air Lasing*, 1st ed.; Polynkin, P., Cheng, Y., Eds.; Springer Series in Optical Sciences 208; Springer: Cham, Switzerland, 2018; pp. 1–18.

20. Yuan, L.; Liu, Y.; Yao, J.; Cheng, Y. Recent advances in air lasing: A perspective from quantum coherence. *Adv. Quantum Technol.* **2019**, *2*, 1900080. [CrossRef]

21. Yao, J.; Jiang, S.; Chu, W.; Zeng, B.; Wu, C.; Lu, R.; Li, Z.; Xie, H.; Li, G.; Yu, C.; et al. Population redistribution among multiple electronic states of molecular nitrogen ions in strong laser fields. *Phys. Rev. Lett.* **2016**, *116*, 143007. [CrossRef]

22. Richter, M.; Lytova, M.; Morales, F.; Haessler, S.; Smirnova, O.; Spanner, M.; Ivanov, M. Rotational quantum beat lasing without inversion. *Optica* **2020**, *7*, 586–592. [CrossRef]

23. Zhang, Q.; Xie, H.; Li, G.; Wang, X.; Lei, H.; Zhao, J.; Chen, Z.; Yao, J.; Cheng, Y.; Zhao, Z. Sub-cycle coherent control of ionic dynamics via transient ionization injection. *Commun. Phys.* **2020**, *3*, 50. [CrossRef]

24. Mysyrowicz, A.; Danylo, R.; Houard, A.; Tikhonchuk, V.; Zhang, X.; Fan, Z.; Liang, Q.; Zhuang, S.; Yuan, L.; Liu, Y. Lasing without population inversion in N_2^+. *APL Photonics* **2019**, *4*, 110807. [CrossRef]

25. Britton, M.; Laferriere, P.; Ko, D.H.; Li, Z.; Kong, F.; Brown, G.; Naumov, A.; Zhang, C.; Arissian, L.; Corkum, P.B. Testing the role of recollision in N_2^+ air lasing. *Phys. Rev. Lett.* **2018**, *120*, 133208. [CrossRef] [PubMed]

26. Zhang, H.; Jing, C.; Yao, J.; Li, G.; Zeng, B.; Chu, W.; Ni, J.; Xie, H.; Xu, H.; Chin, S.L.; et al. Rotational coherence encoded in an "air-laser" spectrum of nitrogen molecular ions in an intense laser field. *Phys. Rev. X* **2013**, *3*, 041009. [CrossRef]

27. Liu, Y.; Ding, P.; Lambert, G.; Houard, A.; Tikhonchuk, V.T.; Mysyrowicz, A. Recollision-induced superradiance of ionized nitrogen molecule. *Phys. Rev. Lett.* **2015**, *115*, 133203. [CrossRef] [PubMed]

28. Britton, M.; Lytova, M.; Laferrière, P.; Peng, P.; Morales, F.; Ko, D.H.; Richter, M.; Polynkin, P.; Villeneuve, D.M.; Zhang, C.; et al. Short- and long-term gain dynamics in N_2^+ air lasing. *Phys. Rev. A* **2019**, *100*, 013406. [CrossRef]

29. Li, G.; Jing, C.; Zeng, B.; Xie, H.; Yao, J.; Chu, W.; Ni, J.; Zhang, H.; Xu, H.; Cheng, Y.; et al. Signature of superradiance from a nitrogen-gas plasma channel produced by strong-field ionization. *Phys. Rev. A* **2014**, *89*, 033833. [CrossRef]

30. Borri, P.; Langbein, W.; Hvam, J.M.; Heinrichsdorff, F.; Mao, M.-H.; Bimberg, D. Ultrafast gain dynamics in InAs–InGaAs quantum-dot amplifiers. *IEEE Photonics Technol. Lett.* **2000**, *12*, 594–596. [CrossRef]

31. Wang, Y.; Wang, S.; Oliva, E.; Li, L.; Berrill, M.; Yin, L.; Nejdl, J.; Luther, B.M.; Proux, C.; Le, T.T.; et al. Gain dynamics in a soft-X-ray laser amplifier perturbed by a strong injected X-ray field. *Nat. Photonics* **2014**, *8*, 381–384. [CrossRef]

32. Zhang, A.; Liang, Q.; Lei, M.; Yuan, L.; Liu, Y.; Fan, Z.; Zhang, X.; Zhuang, S.; Wu, C.; Gong, Q.; et al. Coherent modulation of superradiance from nitrogen ions pumped with femtosecond pulses. *Opt. Express* **2019**, *27*, 12638–12646. [CrossRef]

33. Chen, J.; Yao, J.; Zhang, H.; Liu, Z.; Xu, B.; Chu, W.; Qiao, L.; Wang, Z.; Fatome, J.; Faucher, O.; et al. Electronic-coherence-mediated molecular nitrogen-ion lasing in a strong laser field. *Phys. Rev. A* **2019**, *100*, 031402. [CrossRef]

34. Maki, J.J.; Malcuit, M.S.; Raymer, M.G.; Boyd, R.W.; Drummond, P.D. Influence of collisional dephasing process on superfluorescence. *Phys. Rev. A* **1989**, *40*, 5135. [CrossRef] [PubMed]

35. Yuan, L.; Hokr, B.H.; Traverso, A.J.; Voronine, D.V.; Rostovtsev, Y.; Sokolov, A.V.; Scully, M. Theoretical analysis of the coherence-brightened laser in air. *Phys. Rev. A* **2013**, *87*, 023826. [CrossRef]

36. Carlson, N.W.; Jackson, D.J.; Schawlow, A.L.; Gross, M. Superradiance triggering spectroscopy. *Opt. Commun.* **1980**, *32*, 350–354. [CrossRef]

37. MacGillivary, J.C.; Feld, M.S. Theory of superradiance in an extended, optically thick medium. *Phys. Rev A* **1976**, *14*, 1169. [CrossRef]